arXiv:1506.03060v3 [nlin.CD] 5 Nov 2015

High-low frequency slaving and regularity issues in the $3D$ Navier-Stokes equations

J. D. Gibbon[1]

Department of Mathematics, Imperial College London, SW7 2AZ, UK

Abstract

The old idea that an infinite dimensional dynamical system may have its high modes or frequencies slaved to low modes or frequencies is re-visited in the context of the $3D$ Navier-Stokes equations. A set of dimensionless frequencies $\{\tilde{\Omega}_m(t)\}$ are used which are based on L^{2m}-norms of the vorticity. To avoid using derivatives a closure is assumed that suggests that the $\tilde{\Omega}_m$ $(m > 1)$ are slaved to $\tilde{\Omega}_1$ (the global enstrophy) in the form $\tilde{\Omega}_m = \tilde{\Omega}_1 \mathcal{F}_m(\tilde{\Omega}_1)$. This is shaped by the constraint of two Hölder inequalities and a time average from which emerges a form for $\mathcal{F}_m$ which has been observed in previous numerical Navier-Stokes and MHD simulations. When written as a phase plane in a scaled form, this relation is parametrized by a set of functions $1 \leq \lambda_m(\tau) \leq 4$, where curves of constant λ_m form the boundaries between tongue-shaped regions. In regions where $2.5 \leq \lambda_m \leq 4$ and $1 \leq \lambda_m \leq 2$ the Navier-Stokes equations are shown to be regular : numerical simulations appear to lie in the latter region. Only in the central region $2 < \lambda_m < 2.5$ has no proof of regularity been found.

Dedicated to the memory of David Broomhead (1950 − 2014)

1 Introduction

1.1 Historical background

A generation ago a recurrent theme in studies in infinite dimensional dynamical systems was the idea that a small subset of low modes or coherent states might conceivably control the dynamics by slaving the higher modes to this subset. Having originally emerged from earlier work on centre manifolds in studies in ordinary differential equations (Broomhead, Indik, Newell and Rand (1991), Guckenheimer and Holmes (1997), Holmes, Lumley and Berkooz (1996)), such ideas obviously have a lasting appeal, particularly for those who work in turbulent flows where the number of degrees of freedom are so large that resolved computations at realistic Reynolds numbers are hard to achieve : see Moin and Mahesh (1998), Donzis, Young and Sreenivasan (2008), Pandit, Perlekar and Ray (2009), Ishihara, Gotoh and Kaneda (2009), Kerr (2012, 2013) and Schumacher, Scheelb, Krasnov, Donzis, Yakhot and Sreenivasan (2014). For partial differential equations there also emerged a parallel and closely related body of work on global attractors and inertial manifolds which aimed to prove the finite dimensionality of the system in question in some specified sense : Foias, Sell and Temam (1988), Titi (1990), Foias and Titi (1991), Robinson (1996), Foias, Manley, Rosa and Temam (2001). Some success was achieved for the one-dimensional the Kuramoto-Sivashinsky equation where an inertial manifold was proved to exist (Foias, Jolly, Kevrekidis, Sell and Titi 1988). Further success was also achieved for the $2D$ incompressible Navier-Stokes equations when a global attractor was shown to exist with a sharp estimate for its dimension (Constantin, Foias and Temam 1988), with further estimates on the number of determining modes and nodes : see Foias and Prodi (1967), Foias and Temam (1984), Jones and Titi (1993), Olson and Titi (2003) and Farhat, Jolly and Titi (2014).

The aim of this paper is to revisit the low/high mode idea in a new way in the context of the open question of the global regularity of the $3D$ Navier-Stokes equations

$$\partial_t \boldsymbol{u} + \boldsymbol{u} \cdot \nabla \boldsymbol{u} = \nu \Delta \boldsymbol{u} - \nabla p + \boldsymbol{f}(\boldsymbol{x}), \qquad \operatorname{div} \boldsymbol{u} = \operatorname{div} \boldsymbol{f} = 0, \qquad (1.1)$$

with periodic boundary conditions on a cube of volume $\mathcal{V} = [0, L]^3_{per}$. The body force $\boldsymbol{f}(\boldsymbol{x})$ is taken to be L^2-bounded and centred around a forcing length scale ℓ in the manner described by

---

Doering and Foias (2002) : in this paper ℓ is taken as $\ell = L$ for convenience. The two dimensionless numbers corresponding to the forcing and the system response are respectively given by the Grashof and Reynolds numbers

$$Gr = \frac{L^{3/2}\|\boldsymbol{f}\|_2}{\nu^2} \qquad\qquad Re = \frac{LU_0}{\nu} \qquad\qquad (1.2)$$

where $U_0^2 = L^{-3}\left\langle \|\boldsymbol{u}\|_2^2 \right\rangle_T$ with $\|\cdot\|_2$ representing the L^2-norm and $\langle\cdot\rangle_T$ a time average up to time $T > 0$.

1.2   Some recent analytical and numerical scaling results

Given the open nature of the question of global regularity of solutions of the $3D$ Navier-Stokes equations, analyses have conventionally been based on an assumption of some type. The main one has been that the velocity field is assumed to remain bounded in some function space, the best being the $u \in L^3(\mathcal{V})$ result of Escauriaza, Seregin and Sverák (2003). An alternative computational approach has been to discuss low modes in terms of coherent states by projecting onto special selections of Fourier-Galerkin modes (Broomhead, Indik, Newell and Rand (1991), Holmes, Lumley and Berkooz (1996)).

Here we break with both of these traditions and instead introduce a set of time dependent frequencies or inverse time scales (or 'modes')

$$\{\Omega_1(t),\ \Omega_2(t),\ \dots\ \Omega_m(t)\}\,, \qquad\qquad (1.3)$$

based on L^{2m}-norms of the three-dimensional vorticity field $\boldsymbol{\omega}(\boldsymbol{x},\,t)$ which obeys

$$(\partial_t + \boldsymbol{u}\cdot\nabla)\,\boldsymbol{\omega} = \nu\Delta\boldsymbol{\omega} + \boldsymbol{\omega}\cdot\nabla\boldsymbol{u} + \operatorname{curl}\boldsymbol{f}\,. \qquad\qquad (1.4)$$

The Ω_m in (1.3) are defined such that each has the dimension of a frequency

$$\Omega_m(t) = \left(L^{-3}\int_{\mathcal{V}}|\boldsymbol{\omega}|^{2m}\,dV\right)^{1/2m}. \qquad\qquad (1.5)$$

$\Omega_1(t)$ is the global enstrophy and the $\Omega_m(t)$ are higher moments. The set (1.3) would be widely spread if the vector field $\boldsymbol{\omega}(\boldsymbol{x},\,t)$ is strongly intermittent, whereas they would be squeezed closely together if $\boldsymbol{\omega}$ is mild in behaviour. Multiplication by the inverse of the constant frequency $\varpi_0 = \nu L^{-2}$ produces a non-dimensional set $\tilde{\Omega}_m = \varpi_0^{-1}\Omega_m$.

In earlier work, a scaled set of the $\tilde{\Omega}_m$

$$D_m = \tilde{\Omega}_m^{\alpha_m} \qquad \text{with} \qquad \alpha_m = \frac{2m}{4m-3}\,, \qquad\qquad (1.6)$$

was shown to have bounded time averages for $1 \le m \le \infty$ (Gibbon 2011)

$$\langle D_m\rangle_T \le c\,Re^3 + O\left(T^{-1}\right). \qquad\qquad (1.7)$$

Given that $\alpha_1 = 2$, the first of these, $\langle D_1\rangle_T \le c\,Re^3$, is just the well-known result that the time average of the global enstrophy is a bounded quantity. The origin of the α_m-scaling in (1.6) comes from symmetry considerations.

It was observed in Donzis *et al.* (2013) that time plots of the $D_m(t)$ from several different simulations were ordered on a descending scale. In a further paper (Gibbon *et al.* 2014), it was observed that plots of the maxima in time of $\ln D_m/\ln D_1$ led to the relation

$$D_m \le D_1^{A_{m,\lambda}} \qquad \text{with} \qquad A_{m,\lambda} = \frac{(m-1)\lambda+1}{4m-3}\,, \qquad\qquad (1.8)$$

where the accuracy of the fit lay within 5%. The corresponding fixed values of the fitting parameter λ lay in the range $1.15 \leq \lambda \leq 1.5$. These numerical simulations were: (i) a $1024^2 \times 2048$ decaying calculation with anti-parallel initial conditions at about $Re_\lambda \sim 400$ based on work reported in Kerr (2012, 2013); (ii) a forced and a decaying $(512)^3$ pair of simulations at about $Re_\lambda \sim 250$ – see Gibbon *et al.* (2014); (iii) data from a large-scale statistically steady simulation $(4096)^3$ simulation on 10^5 processors at $Re_\lambda \approx 1000$, reported in Donzis *et al.* (2008, 2010) and Yeung, Donzis and Sreenivasan (2012). In addition to these, (1.8) has also been seen in a set of $3D$-MHD simulations in similar circumstances to those performed for the Navier-Stokes equations: see Gibbon *et al.* (2015).

2   A time-dependent closure avoiding derivatives of ω

The inequality in (1.8) is a numerical observation. To put this, or something close to it, on a rigorous footing for the $3D$ Navier-Stokes equations, the first step is to assume that a strong solution[2] exists on a maximal time interval $[0, T^*)$ on which it is assumed that $\tilde{\Omega}_1$ is bounded – hence all the other $\tilde{\Omega}_m$ are also bounded. Then, instead of taking the standard route of a Sobolev inequality, which involves derivatives of ω, the next step is to postulate a relation between $\tilde{\Omega}_m$ and lower $\tilde{\Omega}_n$ which could be thought of as a high/low frequency closure[3]

$$\tilde{\Omega}_m = F_m(\tilde{\Omega}_1, \tilde{\Omega}_2, \ldots, \tilde{\Omega}_n), \qquad 1 \leq n < m. \qquad (2.1)$$

This closure, which is designed to avoid the introduction of derivatives in ω, must be constrained and shaped by the fact that $\tilde{\Omega}_m$ must not only satisfy Holder's inequality

$$\tilde{\Omega}_1 \leq \ldots \leq \tilde{\Omega}_m \leq \tilde{\Omega}_{m+1} \qquad (2.2)$$

but it must also satisfy a triangular version Hölder's inequality for $m > 1$ (see Appendix A)

$$\left(\frac{\tilde{\Omega}_m}{\tilde{\Omega}_1}\right)^{m^2} \leq \left(\frac{\tilde{\Omega}_{m+1}}{\tilde{\Omega}_1}\right)^{m^2-1}. \qquad (2.3)$$

It is well known that the existence and uniqueness of solutions depends entirely on the bounded of the H_1-norm of the velocity field (Leray 1934), which is proportional to $\tilde{\Omega}_1$. Thus we simplify the dependency of $\tilde{\Omega}_m$ to the first frequency $\tilde{\Omega}_1$ such that our 'closure' in (2.1) is reduced to

$$\tilde{\Omega}_m = \tilde{\Omega}_1 \mathcal{F}_m(\tilde{\Omega}_1). \qquad (2.4)$$

The inequalities (2.2) and (2.3) demand that $\mathcal{F}_m$ must satisfy both

$$\mathcal{F}_{m+1} \geq \mathcal{F}_m^{m^2/(m^2-1)}, \qquad \mathcal{F}_m \geq 1. \qquad (2.5)$$

The first inequality in (2.5) can be further simplified by the substitution

$$\mathcal{F}_m = \left[h_m\left(\tilde{\Omega}_1, \tau\right)\right]^{\frac{m-1}{m}} \qquad (2.6)$$

for a sequence of smooth, arbitrary functions $h_m\left(\tilde{\Omega}_1, \tau\right)$ which must then form a monotonically increasing sequence

$$1 \leq h_m\left(\tilde{\Omega}_1, \tau\right) \leq h_{m+1}\left(\tilde{\Omega}_1, \tau\right). \qquad (2.7)$$

---

[2]We are using the standard contradiction method in PDE-analysis where it is assumed that there exists a maximal interval time $[0, T^*)$ on which solutions of the Navier-Stokes equations exist and are unique: the strategy is to then attempt to prove a contradiction in the limit $t \to T^*$.

[3]Strictly speaking, (2.4) is not a closure in the conventional sense used in turbulence modelling. Rather, it is an expression of how $\tilde{\Omega}_m$ can be related to lower $\tilde{\Omega}_n$, under the constraints (2.2) and (2.3), without resorting to derivatives of ω. Nevertheless, we will continue to use the word 'closure' for convenience.

In (2.6) and (2.7), τ is a dimensionless time $\tau = \varpi_0 t$. Finally, (2.4) is reduced to

$$\tilde{\Omega}_m = \tilde{\Omega}_1 \left[h_m \left(\tilde{\Omega}_1, \tau \right) \right]^{\frac{m-1}{m}} . \tag{2.8}$$

The result depends only on the finiteness of the domain and the inverse box frequency $\varpi_0 = \nu L^{-2}$ to create the dimensionless time τ. The relation (2.8) is no more than an expression of the potentially arbitrarily large distance between $\tilde{\Omega}_m$ and $\tilde{\Omega}_1$ in the form of an equality. In fact, (2.8) contains no $3D$ Navier-Stokes information but once it is considered in this context, the finiteness of the time averages in (1.7) must be enforced. An application of a Hölder inequality to (2.8) shows that the h_m must therefore be constrained by

$$\left\langle h_m^{2/3} \right\rangle_T < \infty . \tag{2.9}$$

One choice of h_m consistent with this is that it cannot be any stronger than a power law in $\tilde{\Omega}_1$

$$h_m \left(\tilde{\Omega}_1, \tau \right) = 1 + \tilde{c}_m \tilde{\Omega}_1^{\lambda_m(\tau)-1} \tag{2.10}$$

where the monotonically increasing[4] λ_m must lie in the range

$$1 \leq \lambda_m(\tau) \leq 4 . \tag{2.11}$$

Morover, the dimensionless constants $\tilde{c}_m$ will be chosen more specifically later. The final result is that if there exists a strong solution on the interval $[0, T^*)$, then with the choice of h_m as in (2.10), there exists a set of exponents $\{\lambda_m(\tau)\}$ such that

$$\tilde{\Omega}_m = \tilde{\Omega}_1 \left[1 + \tilde{c}_m \tilde{\Omega}_1^{\lambda_m(\tau)-1} \right]^{\frac{m-1}{m}} , \qquad 1 < m < \infty . \tag{2.12}$$

In practice $\tilde{\Omega}_1$ is so large that we may safely ignore the factor of unity in $h_m(\tilde{\Omega}_1, \tau)$ in (2.12). With the definition

$$A_{m,\lambda_m(\tau)} = \tfrac{1}{2}\alpha_m \left[1 + (\lambda_m(\tau) - 1) \left(\frac{m-1}{m} \right) \right] = \frac{(m-1)\lambda_m(\tau) + 1}{4m - 3} , \tag{2.13}$$

we have

$$D_m = c_m D_1^{A_{m,\lambda_m(\tau)}} . \tag{2.14}$$

which is a version of (1.8) with $\lambda_m = \lambda_m(\tau)$ as a function of time. The introduction of the set $\{\lambda_m(\tau)\}$ means the dynamics are analyzed in terms of D_1 and $\{\lambda_m(\tau)\}$ instead of D_1 and $\{D_m(\tau)\}$. In (1.8) the inequality is appropriate because in Gibbon et $al.$ (2014) λ_m was estimated as a constant parameter corresponding to maxima in time in plots of $\ln D_m / \ln D_1$ versus time. Note that when $\lambda_m = 4$, $A_{m,4} = 1$, at which point the D_m versus D_1 relation is linear. Beyond the range in (2.11), when $\lambda_m > 4$, (2.14) is no longer valid. Clearly, a further set of numerical experiments are needed to analyze more closely the trajectories of $\lambda_m(\tau)$ in (2.14).

---

[4]In Gibbon et $al.$ (2014), in which only the maxima in time of D_m were considered, there were indications that the λ_m decreased with m, albeit very weakly, which is not consistent with the constraint $\lambda_m \leq \lambda_{m+1}$ that stems from (2.5). This suggests that the choice of h_m made in (2.10) needs a slight modification. This issue needs testing with a proper set of numerical experiments.
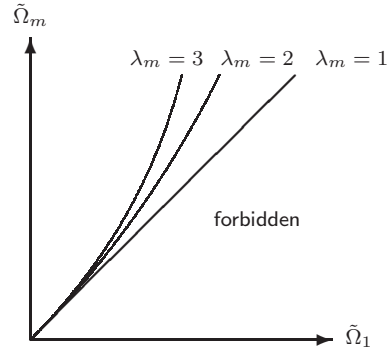
Figure 1: Plots of the convex curves $\tilde{\Omega}_m$ versus $\tilde{\Omega}_1$ for $\lambda_m = 2, \ 3$ lying above the straight line $\lambda_m = 1$. As λ_m increases the $\tilde{\Omega}_m$ spread more, corresponding to greater intermittency in the $\boldsymbol{\omega}$-field.
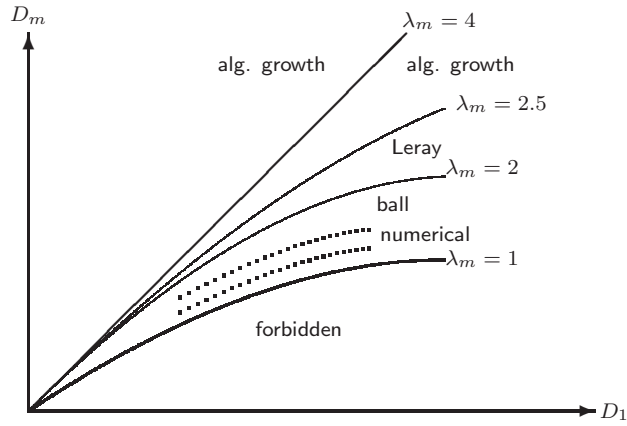

Figure 2: A cartoon in the $D_1 - D_m$ plane parametrized by λ_m : in the region $2.5 \leq \lambda_m \geq 4$ the D_m undergo no more than algebraic growth with a restriction on (large) initial data for $2.5 \leq \lambda_m \leq 4$; in the region $2 < \lambda_m < 2.5$ only Leray's weak solutions are known to exist with the only control over D_m being the bounded long time averages $\langle D_m \rangle_T < \infty$; at $\lambda_m = 2$ the bound on D_1 grows exponentially in time; in the region $1 \leq \lambda_m < 2$ the D_m lie within an absorbing ball. The dotted curves represent the approximate regions of the maxima in the numerical simulations reported in Donzis *et al.* (2013) and Gibbon *et al.* (2014). The region below the curve $\lambda_m = 1$ is forbidden as Hölder's inequality is violated there.

3   Navier-Stokes results in the $D_m - D_1$ plane parametrized by $\lambda_m(\tau)$

The essential idea behind (2.13) has been to avoid the use of derivatives of $\boldsymbol{\omega}$ and instead transfer the dynamical relationship behind $\tilde{\Omega}_m$ and $\tilde{\Omega}_1$ to the $\{\lambda_m(\tau)\}$. This allows us to treat the $D_m - D_1$ phase as a phase plane parametrized by $\lambda_m(\tau)$, as in Fig. 2. The curves of constant λ_m are drawn as concave curves, although actual orbits $\lambda_m(\tau)$ could potentially wander across the phase plane and over these labelled boundaries, even though numerical experiments so far have found that their maxima lie in the lower half of the lowest tongue labelled by the dashed curves. We wish to demonstrate certain results about the nature of solutions in different sectors of this phase plane bounded by curves $\lambda_m = \mathrm{const}$, so in this section λ_m is treated as a constant.

The curve $\lambda_m = 1$ is associated with the lower bound $\tilde{\Omega}_1 \leq \tilde{\Omega}_m$, which translates to

$$D_1^{\alpha_m/2} \leq D_m \qquad \text{where} \qquad A_{m,1} = \alpha_m/2 = \frac{m}{4m-3} \,. \tag{3.1}$$

Thus the regions below the line in Fig. 1 and below the lowest curve in Fig. 2, both corresponding to $\lambda_m = 1$, are forbidden by Hölder's inequality. Moreover, the relation between D_m and D_1 is linear when $\lambda_m = 4$. The results of §3.1 alone can be found in Gibbon *et al.* (2014): the rest of the material is new.

3.1   The region $1 \leq \lambda_m < 2$ and the curve $\lambda_m = 2$

From the definition of the D_m in (1.6) note that $D_1 = L\nu^{-2}\|\boldsymbol{\omega}\|_2^2$. A purely formal differential inequality for D_1 is

$$\tfrac{1}{2}\dot{D}_1 \leq L\nu^{-2}\left\{-\nu\int_{\mathcal{V}}|\nabla\boldsymbol{\omega}|^2\,dV + \int_{\mathcal{V}}|\nabla\boldsymbol{u}||\boldsymbol{\omega}|^2\,dV + L^{-1}\|\boldsymbol{\omega}\|_2\|\boldsymbol{f}\|_2\right\}. \qquad (3.2)$$

Dealing with the negative term first, an integration by parts gives

$$\int_{\mathcal{V}}|\boldsymbol{\omega}|^2\,dV \leq \left(\int_{\mathcal{V}}|\nabla\boldsymbol{\omega}|^2 dV\right)^{1/2}\left(\int_{\mathcal{V}}|\boldsymbol{u}|^2 dV\right)^{1/2}, \qquad (3.3)$$

where the dimensionless energy E is defined as

$$E = \nu^{-2}L^{-1}\int_{\mathcal{V}}|\boldsymbol{u}|^2\,dV. \qquad (3.4)$$

This is always bounded such that

$$\overline{\lim}_{t\to\infty}E \leq c\,Gr^2. \qquad (3.5)$$

Next, the nonlinear term in (3.2) needs to be estimated. The standard result using a Sobolev inequality produces a cubic nonlinearity D_1^3 that is too strong for the negative term: all that can be deduced from this is that D_1 is bounded from above only for short times or for small initial data. The difficulty caused by this term has been known for many decades: see Constantin and Foias (1988) and Foias *et al.* (2001). We circumvent this problem by proceeding as follows:

$$\begin{aligned}
\int_{\mathcal{V}}|\nabla\boldsymbol{u}||\boldsymbol{\omega}|^2 dV &= \int_{\mathcal{V}}|\boldsymbol{\omega}|^{\frac{2m-3}{m-1}}|\boldsymbol{\omega}|^{\frac{1}{m-1}}|\nabla\boldsymbol{u}|dV \\
&\leq \left(\int_{\mathcal{V}}|\boldsymbol{\omega}|^2 dV\right)^{\frac{2m-3}{2(m-1)}}\left(\int_{\mathcal{V}}|\boldsymbol{\omega}|^{2m}dV\right)^{\frac{1}{2m(m-1)}}\left(\int_{\mathcal{V}}|\nabla\boldsymbol{u}|^{2m}dV\right)^{\frac{1}{2m}} \\
&\leq C_m\left(\int_{\mathcal{V}}|\boldsymbol{\omega}|^2 dV\right)^{\frac{2m-3}{2(m-1)}}\left(\int_{\mathcal{V}}|\boldsymbol{\omega}|^{2m}dV\right)^{\frac{1}{2(m-1)}} \\
&= C_m L^3 \varpi_0^3 D_1^{\frac{2m-3}{2m-2}}D_m^{\frac{4m-3}{2m-2}}, \qquad 1 < m < \infty.
\end{aligned} \qquad (3.6)$$

The penultimate line is based on $\|\nabla\boldsymbol{u}\|_p \leq c_p\|\boldsymbol{\omega}\|_p$, for $1 < p < \infty$. Inserting the depletion $D_m = c_{1,m}D_1^{A_{m,\lambda_m}}$ gives

$$L\nu^{-2}\int_{\mathcal{V}}|\nabla\boldsymbol{u}||\boldsymbol{\omega}|^2\,dV \leq c_{2,m}\varpi_0\,D_1^{\xi_m}, \qquad (3.7)$$

where ξ_m is defined as

$$\xi_m = \frac{A_{m,\lambda_m}(4m-3) + 2m - 3}{2(m-1)}. \qquad (3.8)$$

It can now be seen that by using (1.8), the m-dependency cancels leaving[5]

$$\xi_m = 1 + \tfrac{1}{2}\lambda_m. \qquad (3.9)$$

ξ_m does not reach its conventional value of 3 unless $\lambda_m = 4$. The differential inequality (3.2) now becomes ($\tau = \varpi_0 t$)

$$\tfrac{1}{2}\frac{dD_1}{d\tau} \leq -\frac{D_1^2}{E} + c_{2,m}D_1^{1+\frac{1}{2}\lambda_m} + GrD_1^{1/2}. \qquad (3.10)$$

---

[5]Lu and Doering (2008) showed numerically that by maximizing the enstrophy subject to div $\boldsymbol{u} = 0$, two branches of the nonlinear term appear, the lower being $D_1^{1.78}$ and the upper $D_1^{2.997}$. Later, Schumacher, Eckhardt and Doering (2010), suggested that $7/4$ and 3 were the likely values of these two exponents: the exponent $1 + \frac{1}{2}\lambda_m = 7/4$ corresponds to $\lambda_m = 1.5$ which lies at the upper end of the range $1.15 \leq \lambda_m \leq 1.5$ observed in Gibbon *et al.* (2014).

Given that E is bounded above, D_1 is always under control provided λ_m is restricted to the range $1 \leq \lambda_m < 2$. Formally, there exists an absorbing ball for D_1 of radius

$$\overline{\lim}_{t\to\infty} D_1 \leq \tilde{c}_{2,m} Gr^{\frac{4}{2-\lambda_m}} + O\left(Gr^{4/3}\right), \tag{3.11}$$

It has been shown in Gibbon *et al.* (2014) that this gives rise to a global attractor $\mathcal{A}$ whose Lyapunov dimension has been estimated as

$$d_L(\mathcal{A}) \leq \begin{cases} c_{4,m} Re^{\frac{3}{5}\left(\frac{6-\lambda_m}{2-\lambda_m}\right)} \\ c_{5,m} Gr^{\frac{3}{5}\left(\frac{4-\lambda_m}{2-\lambda_m}\right)} \end{cases} \tag{3.12}$$

depending on whether one chooses to use the Reynolds or Grashof number. In the limit $\lambda_m \to 2$ the radius of the ball in (3.11) grows but, at $\lambda_m = 2$, the finiteness of $\int_0^t D_1(\tau)d\tau$ means that $D_1(t)$ has an exponentially growing upper bound.

3.2 The regions $2.5 \leq \lambda_m \leq 4$

It has also been shown in Gibbon (2012) and Gibbon *et al.* (2014) that the D_m satisfy the differential inequality for $1 < m < \infty$

$$\dot{D}_m \leq D_m^3 \left(-\varpi_{1,m}\left(\frac{D_m}{D_1}\right)^{\eta_m} + \varpi_{2,m}\right) + \varpi_{3,m} Gr D_m^{1-1/\alpha_m}, \tag{3.13}$$

where $\eta_m = 2m/3(m-1)$ and where $\varpi_{1,m} < \varpi_{2,m}$ are constant frequencies. The last (forcing) term, is hard to handle in conjunction with the others so this will be separated and dealt with last: no more than algebraic growth in time can come from it. Let us now divide (3.13) by D_m^3 to obtain

$$\tfrac{1}{2}\frac{d}{dt} D_m^{-2} \geq \varpi_{1,m} X_m(t) D_m^{-2} - \varpi_{2,m} \tag{3.14}$$

where

$$X_m = D_m^2 \left(\frac{D_m}{D_1}\right)^{\eta_m}. \tag{3.15}$$

A bound away from zero of the time integral of $X_m(t)$ is required to show that $D_m^{-2}(t)$ never passes through zero for some range of initial conditions. To achieve this we introduce the nonlinear depletion as in (1.6). Noting that $\eta_m + 2 = 2(4m-3)/3(m-1) = 2\eta_m \alpha_m^{-1}$, it is found that ($\tilde{c}_m = c_m^{2+\eta_m}$)

$$\begin{aligned} X_m &= \tilde{c}_m D_1^{\eta_m(\lambda_m-1)(m-1)/m} \\ &= \tilde{c}_m D_1^{2(\lambda_m-1)/3}. \end{aligned} \tag{3.16}$$

It is at this point that we introduce the lower bound[6] on $\int_0^t D_1(t')\,dt'$ found in Doering and Foias (2002)

$$\int_0^t D_1(t')\,dt' \geq t\,Gr + O(t^{-1}). \tag{3.17}$$

---

[6]Doering and Foias (2002) have shown that there are two estimates for the lower bound to the integral in (3.17). The first is proportional to $t\,Gr$ and the second to $t\,Gr^2 Re^{-2}$ depending on the relative sizes of the forcing length scale ℓ and the Taylor micro-scale. The first has been derived using a Poincaré inequality so it is likely to be less sharp although the two coincide when the bound $Gr \leq c\,Re^2$ is saturated. For simplicity we use the Gr-bound.

This comes into play only if $2(\lambda_m - 1)/3 \geq 1$, in which case $\lambda_m \geq 5/2$, where we can then use a Schwarz inequality to obtain

$$
\int_0^t X_m(t')\, dt' \geq \tilde{c}_m \left(\int_0^t D_1\, dt' \right)^{2(\lambda_m-1)/3} t^{1-2(\lambda_m-1)/3}
$$
$$
\geq t\, \tilde{c}_m Gr^{2(\lambda_m-1)/3} + O\left(t^{1-4(\lambda_m-1)/3} \right) .
$$
(3.18)

(3.14) can be solved to give

$$
\tfrac{1}{2}[D_m(t)]^2 \leq \frac{\exp\{-\varpi_{1,m} \int_0^t X_m(t')\, dt'\}}{\tfrac{1}{2}[D_m(0)]^{-2} - \varpi_{2,m} \int_0^t \exp\{-\varpi_{1,m} \int_0^{t'} X_m(t'')\, dt''\} dt'}
$$
$$
= \frac{\exp\{-c_m \varpi_{1,m} t Gr^{2(\lambda_m-1)/3}\}}{\tfrac{1}{2}[D_m(0)]^{-2} - \varpi_{2,m} \left[\tilde{c}_m \varpi_{1,m} Gr^{2(\lambda_m-1)/3} \right]^{-1} \left(1 - \exp\{-\tilde{c}_m \varpi_{1,m} t\, Gr^{2(\lambda_m-1)/3}\} \right)} .
$$
(3.19)

(3.19) cannot develop a zero in the denominator if

$$
D_m(0) \leq \left(\tfrac{1}{2} \tilde{c}_m \varpi_{1,m} \varpi_{2,m}^{-1} \right)^{1/2} Gr^{(\lambda_m-1)/3} ,
$$
(3.20)

for any $5/2 \leq \lambda_m \leq 4$, in which case the solution decays exponentially. This initial data is not small but it is not huge either. The estimates above have been achieved by neglecting the forcing term in (3.13). The effect of this term on its own yields

$$
D_m(t) \leq [\alpha_m \varpi_{3,m} Gr\, (t_0 + t)]^{\alpha_m} .
$$
(3.21)

3.3   The region $2 < \lambda_m < 2.5$

The dynamics in the middle tongue-shaped region bounded by the two central curves $\lambda_m = 2$ and $\lambda_m = 2.5$ in Fig. 2 remains open. Neither the depletion of nonlinearity nor the increase in dissipation afforded by (2.14) are strong enough so we must fall back on the existence of Leray's weak solutions. The lower bound of Doering and Foias (2002) on the time integral of the enstrophy can only be used on the time integral (see (3.18)

$$
\int_0^t D_1^{2(\lambda_m-1)/3}\, dt'
$$
(3.22)

when $\lambda_m \geq 2.5$. For the range $2 < \lambda_m < 2.5$ the dimensionless energy E can instead be used to bound (3.22) below, but if it passes close to zero for long enough, in the manner of a homoclinic orbit, then the resulting lower bound may be too small to be of use. However, (3.22) could be estimated numerically to monitor its behaviour.

3.4   The region $\lambda_m \geq 4$

The relation between D_m and D_1 expressed in (2.14) is valid only for $1 \leq \lambda_m \leq 4$. At $\lambda_m = 4$ the relation is linear; namely $D_m = c_m D_1$. For the region

$$
D_m \geq c_m D_1
$$
(3.23)

we can insert this relation directly into (3.13) and, provided the c_m in (2.14) are chosen such that $c_m \geq \varpi_{2,m} \varpi_{1,m}^{-1}$, (3.13) reduces to

$$
\dot{D}_m \leq \varpi_{3,m} Gr D_m^{1-1/\alpha_m} ,
$$
(3.24)

yielding the same bound for $D_m(t)$ as in (3.21).

4 Conclusion

Subject to the closure relation (2.14), in which the effect of the higher scaled norms D_m is hidden in the evolution of the set of functions $\lambda_m(\tau)$, it has been shown that the $3D$ Navier-Stokes equations are regular in each of the regions when $\lambda_m \geq 1$, with the exception of the region $2 < \lambda_m < 2.5$. There is also the proviso that initial data is limited in the range $2.5 < \lambda_m \leq 4$. For initial data set in the region $\lambda_m \geq 4$ (above the straightline in Fig 2), the dynamics are no worse than algebraic growth, although such initial data is highly pathological. These results are summarized in Fig. 2. The three regular regions are fundamentally different. Solutions lying in the region $\lambda_m \geq 2.5$ seem moribund in the sense that the forcing dominates only algebraically. However, solutions in the lower region or tongue $1 \leq \lambda_m < 2$ live in an absorbing ball, the radius of which is given in (3.11), and it is here where all the interesting dynamics lies. It has been shown in Gibbon *et al* (2014) that solutions here have a corresponding spectrum that is consistent with statistical turbulence theories : see Frisch (1995) and Doering and Gibbon (2002). As drawn in Fig. 2 (dotted curves), the large-scale numerical simulations reported in Gibbon *et al.* (2014) lie well within this region. This is only partially satisfactory (see below) in the sense that the existence of an absorbing ball is enough for the existence of a global attractor *provided the solution trajectory $\lambda_m(\tau)$ remains in this region*. There are two alternatives :

1. Orbits that originate in the range $1 \leq \lambda_m \leq 2$ always remain there ;

2. Orbits originating in the range $1 \leq \lambda_m \leq 2$ could travel out of this region and into the range $2 < \lambda_m < 2.5$ and beyond. However, the nature of this transition is uncertain, and it is unclear what the nature of weak solutions would mean numerically if this happened.

The numerical simulations performed so far have all had their initial data resting in $1 \leq \lambda_m \leq 2$ and have shown no evidence for the behaviour in item 2. In fact, the observed range $1.15 \leq \lambda_m \leq 1.5$ indicates relatively mild dynamics. Unless a rigorous proof is found for the behaviour in item 1, the possibility that the behaviour in item 2 could occur for higher values of Re ought to be kept in mind. A series of numerical experiments are needed with initial conditions set in the four different regions which track the evolution of $\lambda_m(\tau)$ although in the scaled time $\tau = \varpi_0 t$, ϖ_0 could be so small that one may have to compute for significantly large values of the real time t. If the behaviour in item 2 is observed this would open the question of the physical manifestation of weak solutions. Given that these solutions lack uniqueness, would there be there a corresponding physical effect, such as multiple branching of the λ_m-trajectories?

Acknowledgment

A The triangular Hölder inequality (2.3)

Consider the definition of Ω_m

$$L^3\Omega_m^{2m} = \int_{\mathcal{V}} |\boldsymbol{\omega}|^{2m}\, dV \equiv \int_{\mathcal{V}} |\boldsymbol{\omega}|^{2\alpha}|\boldsymbol{\omega}|^{2\beta} dV \tag{A.1}$$

where $\alpha + \beta = m$. Then, for $m > 1$ and $1 \leq p \leq m - 1$ and $q > 0$, we have

$$L^3\Omega_m^{2m} \leq \left(\int_{\mathcal{V}} |\boldsymbol{\omega}|^{2(m-p)}\, dV\right)^{\frac{\alpha}{m-p}} \left(\int_{\mathcal{V}} |\boldsymbol{\omega}|^{2(m+q)} dV\right)^{\frac{\beta}{m+q}} \tag{A.2}$$

where $\frac{\alpha}{m-p} + \frac{\beta}{m+q} = 1$. Solving for $\alpha, \ \beta$ gives

$$\alpha = \frac{q(m-p)}{p+q} \qquad \text{and} \qquad \beta = \frac{p(m+q)}{p+q}, \tag{A.3}$$

thereby giving

$$\Omega_m^{m(p+q)} \leq \Omega_{m-p}^{q(m-p)} \Omega_{m+q}^{p(m+q)}. \tag{A.4}$$

Now choose $q = 1$ and $p = m - 1$ to obtain

$$\Omega_m^{m^2} \leq \Omega_1 \Omega_{m+1}^{m^2-1}, \tag{A.5}$$

which leads to (2.3).

References

[1] Broomhead, D. S., Indik, R., Newell, A. C. & Rand, D. A. (1991) Local adaptive Galerkin bases for large-dimensional dynamical systems. *Nonlinearity*, **4**, 159–197.

[2] Constantin, P. & Foias, C. (1988) *The Navier-Stokes equations*. Chicago University Press, Chicago, USA.

[3] Constantin P., Foias, C. & Temam R. (1988) On the dimension of the attractors in two-dimensional turbulence. *Physica D*, **30**, 284–296.

[4] Doering, C. R. & Foias, C. (2002) Energy dissipation in body-forced turbulence. *J. Fluid Mech.* **467**, 289–306.

[5] Doering, C. R. & Gibbon, J. D. (2002) Bounds on moments of the energy spectrum for weak solutions of the $3D$ Navier-Stokes equations, *Physica D*, **165**, 163–175.

[6] Donzis, D., Gibbon, J. D., Gupta, A., Kerr, R. M., Pandit, R. & Vincenzi, D. (2013) Vorticity moments in four numerical simulations of the $3D$ Navier-Stokes equations. *J. Fluid Mech.*, **732**, 316–331.

[7] Donzis, D. & Yeung, P. K. (2010) Resolution effects and scaling in numerical simulations of passive scalar mixing in turbulence. *Physica* D, **239**, 1278–1287.

[8] Donzis, D., Yeung, P. K. & Sreenivasan, K. R. (2008) Dissipation and enstrophy in isotropic turbulence : scaling and resolution effects in direct numerical simulations. *Phys. Fluids*, **20**, 045108.

[9] Escauriaza, L., Seregin, G. & Sverák, V. (2003) L^3-solutions to the Navier-Stokes equations and backward uniqueness. *Russ. Math. Surveys*, **58**, 211–250.

[10] Farhat, A., Jolly, M. S. & Titi, E. S. (2014) *Continuous data assimilation for 2D Bénard convection through velocity measurements alone.* arXiv:1410.1767v1.

[11] Foias, C., Jolly, M. S., Kevrekidis, I. G., Sell, G. R. & Titi, E. S. (1988) On the computation of inertial manifolds. *Phys. Lett. A*, **131**, 433–436.

[12] Foias, C., Manley, O., Rosa, R. & Temam, R. (2001) *Navier-Stokes equations and turbulence*. Cambridge University Press, Cambridge, UK.

[13] Foias, C. & Prodi, G. (1967) Sur le comportement global des solutions non stationnaires des équations de Navier-Stokes en dimension two. *Rend. Sem. Mat. Univ. Padova*, **39**, 1–34.

[14] Foias, C., Sell, G. R. & Temam, R. (1988) Inertial manifolds for nonlinear evolutionary equations. *J. Diff. Equ.*, **73**, 309–353.

[15] Foias, C. & Temam, R. (1984) Determination of the solutions of the Navier-Stokes equations by a set of nodal values. *Math Comp.*, **43**, 117–133.

[16] Foias, C. & Titi, E. S. (1991) Determining nodes, finite difference schemes and inertial manifolds. *Nonlinearity* **4**, 135–153.

[17] Frisch, U. (1995) *Turbulence : the legacy of A. N. Kolmogorov*. Cambridge University Press, UK.

[18] Gibbon, J. D. (2011) A hierarchy of length scales for weak solutions of the three-dimensional Navier–Stokes equations. *Comm. Math. Sci.*, **10**, 131–136.

[19] Gibbon, J. D. (2012) Conditional regularity of solutions of the three dimensional Navier–Stokes equations and implications for intermittency. *J. Math. Phys.*, **53**, 115608.

[20] Gibbon, J. D., Donzis, D., Gupta, A., Kerr, R. M., Pandit, R. & Vincenzi, D. (2014) Regimes of nonlinear depletion and regularity in the $3D$ Navier-Stokes equations. *Nonlinearity*, **27**, 2605–2625.

[21] Gibbon, J., Gupta, A., Krstulovic, G., Pandit, R., Politano, H., Ponty, Y., Pouquet, A., Sahoo, G. & Stawarz J. (2015) *Depletion of Nonlinearity in Magnetohydrodynamic Turbulence : Insights from Analysis and Simulations*, arXiv:1508.03756v2 [physics.flu-dyn].

[22] Guckenheimer, J. & Holmes, P. (1997) *Nonlinear Oscillations, Dynamical Systems, and Bifurcations of Vector Fields*. Applied Mathematical Sciences **42**, Springer-Verlag, Berlin.

[23] Holmes, P., Lumley, J. L. & Berkooz, G. (1996) *Turbulence, Coherent Structures, Dynamical Systems and Symmetry*. Cambridge University Press, UK.

[24] Ishihara T., Gotoh, T. & Kaneda, Y. (2009) Study of high-Reynolds number isotropic turbulence by direct numerical simulation. *Annu. Rev. Fluid Mech.*, **41**, 16–180.

[25] Jones, D. A. & Titi, E. S. (1993) Upper Bounds on the number of determining modes, nodes, and volume elements for the Navier-Stokes equations. *Indiana Univ. Math. J.*, **42**, 875–887.

[26] Kerr, R. M. (2012) Dissipation and enstrophy statistics in turbulence : Are the simulations and mathematics converging? *J. Fluid Mech.*, **700**, 1–4.

[27] Kerr, R. M. (2013) Swirling, turbulent vortex rings formed from a chain reaction of reconnection events. *Phys. Fluids*, **25**, 065101.

[28] Leray, J. (1934) On the motion of a viscous liquid filling space. *Acta Mathematica*, **6**, 193–248.

[29] Lu, L. & Doering, C. R. (2008) Limits on Enstrophy Growth for Solutions of the Three-dimensional Navier-Stokes Equations. *Indiana Univ. Math. J.*, **57**, 2693–2727.

[30] Moin, P. & Mahesh, K. (1998) Direct Numerical Simulation : A Tool for Turbulence Research. *Annu. Rev. Fluid Mech.*, **30**, 539–578.

[31] Olson, E. & Titi, E. S. (2003) Determining modes for continuous data assimilation in 2D turbulence. *J. Statist. Phys.*, **113**, no. 5-6, 799–840.

[32] Pandit, R., Perlekar, P. & Ray, S. S. (2009) Statistical properties of turbulence : an overview. *Pramana J. Phys.*, **73**, 157–191.

[33] Robinson, J. C. (1996) The asymptotic completeness of inertial manifolds. *Nonlinearity*, **9**, 132–1340.

[34] Schumacher, J., Scheelb, J. D., Krasnov, D., Donzis, D., Yakhot, V. & Sreenivasan, K. R. (2014) Small-scale universality in fluid turbulence. *Proc. Nat. Acad. Sci.*, **111**, 10961.

[35] Schumacher, J., Eckhardt, B. & Doering, C. R. (2010) Extreme vorticity growth in Navier-Stokes turbulence. *Phys. Lett. A*, **374**, 861–865.

[36] Titi, E. S. (1990) On approximate Inertial Manifolds to the Navier-Stokes equations. *J. Math. Anal. Appln.*, **149**, 540–557.

[37] Yeung, P. K., Donzis, D. & Sreenivasan, K. R. (2012) Dissipation, enstrophy and pressure statistics in turbulence simulations at high Reynolds numbers. *J. Fluid Mech.*, **700**, 5–15.